



This is a repository copy of *Synthesis and mechanical properties of double cross-linked gelatin-graphene oxide hydrogels*.

White Rose Research Online URL for this paper:  
<http://eprints.whiterose.ac.uk/114835/>

Version: Accepted Version

---

**Article:**

Piao, Y. and Chen, B. (2017) Synthesis and mechanical properties of double cross-linked gelatin-graphene oxide hydrogels. *International Journal of Biological Macromolecules*, 101. pp. 791-798. ISSN 0141-8130

<https://doi.org/10.1016/j.ijbiomac.2017.03.155>

---

**Reuse**

This article is distributed under the terms of the Creative Commons Attribution-NonCommercial-NoDerivs (CC BY-NC-ND) licence. This licence only allows you to download this work and share it with others as long as you credit the authors, but you can't change the article in any way or use it commercially. More information and the full terms of the licence here: <https://creativecommons.org/licenses/>

**Takedown**

If you consider content in White Rose Research Online to be in breach of UK law, please notify us by emailing [eprints@whiterose.ac.uk](mailto:eprints@whiterose.ac.uk) including the URL of the record and the reason for the withdrawal request.



[eprints@whiterose.ac.uk](mailto:eprints@whiterose.ac.uk)  
<https://eprints.whiterose.ac.uk/>

# Synthesis and Mechanical Properties of Double Cross-linked Gelatin-Graphene Oxide Hydrogels

Yongzhe Piao, Biqiong Chen\*

Department of Materials Science and Engineering, University of Sheffield, Mappin Street, Sheffield S1 3JD, United Kingdom

\*Corresponding author. Email: [biqiong.chen@sheffield.ac.uk](mailto:biqiong.chen@sheffield.ac.uk)

## Abstract

Gelatin is an interesting biological macromolecule for biomedical applications. Here, double cross-linked gelatin nanocomposite hydrogels with incorporation of graphene oxide (GO) were synthesized in one pot using glutaraldehyde (GTA) and GTA-grafted GO as double chemical cross-linkers. The nanocomposite hydrogels, in contrast to the neat gelatin hydrogel, exhibited significant increases in mechanical properties by up to 288% in compressive strength, 195% in compressive modulus, 267% in compressive fracture energy and 160% shear storage modulus with the optimal GO concentration. Fourier transform infrared spectroscopy, scanning electron microscopy and swelling tests were implemented to characterize the nanocomposite hydrogels. These hydrogels could have potential in biomedical applications.

**Keywords:** Gelatin, graphene oxide, nanocomposite hydrogel, mechanical properties

## 1. Introduction

Hydrogels, which are soft and comprise a high proportion of water, have been attracting a great deal of attention in the past few decades. They have been widely studied for biomedical applications including tissue engineering and drug delivery because of their similarities to extracellular matrices, excellent biocompatibility, and inherent cellular interaction capability [1-3].

Gelatin is a natural polymer, derived from animal collagen with excellent biocompatibility, affinity to proteins, and biodegradability, as well as low cost [4]. The numerous studies on the gelatin based hydrogels have been reported for biomedical usages such as drug delivery, tissue engineering, gene therapy and biosensing [5,6]. Physical gelatin hydrogels can be obtained by cooling down pre-heated gelatin solutions to below the gelation temperature of ~25 °C (which varies subject to the type of gelatin, concentration, etc.) to trigger the conformational transition from coil to triple helices [7]; however, these hydrogels have poor mechanical properties and low temperature resistance [8,9]. Chemical cross-linking could improve their strength and tune biodegradation rate, but at sacrifice of ductility [5]. Further mechanical improvement is in demand to overcome the limitation for neat gelatin hydrogels to be used in load-bearing applications. There are several approaches to achieving hydrogels with high mechanical performance, for example, copolymer hydrogels, double-network hydrogels and polymer nanocomposite hydrogels [10,11]. Graphene and its derivatives have been considered as effective nanofillers for composite materials [12].

Since it was first reported in 2004, graphene has drawn substantial attention of scientists due to its intriguing properties [13,14]. Graphene oxide (GO), a graphene derivative, exhibits a large surface area, a high aspect ratio, and exceptional mechanical properties, while bearing plenty of oxygen-containing groups on their monolayer two-dimensional sheets [13]. GO can be readily exfoliated and stably dispersed as single-layer sheets in an aqueous solution owing

to its hydrophilic oxygen-containing groups, which is beneficial to prepare mechanically strong nanocomposite hydrogels. These oxygen-containing functional groups enabled GO nanosheets to associate with hydrophilic polymer matrices by physical and chemical interactions to enhance the mechanical performance significantly. For example, the addition of ~5 wt% GO can dramatically increase the compressive strength of poly(N-isopropylacrylamide) (PNIPAM) hydrogels by 3-fold, owing to the interpenetrating network structure comprised of chemically cross-linked PNIPAM and connected GO sheets, as well as the strong intermolecular interaction (hydrogen-bonding) between PNIPAM chains and GO sheets [15].

Through physical and chemical interactions, gelatin (as primary components) and GO formed interesting nanocomposites and nanocomposite hydrogels [16-21]. A strong and bioactive gelatin-GO nanocomposite was reported showing 65%, 84% and 158% increases in the Young's modulus, tensile strength and fracture energy of gelatin, respectively, with the addition of 1 wt% GO [16]. Self-assembled gelatin-GO nanocomposite hydrogels [17] were reported possessing storage moduli of 54–115 kPa at a water content of 98.0–98.5 wt%, and gelatin-reduced graphene oxide nanocomposite hydrogels [18] exhibited storage moduli of 64–172 kPa at a water content of 98.0–98.8 wt%. These hydrogels were formed without an organic cross-linking agent, where graphene was used as a physical cross-linker in the former and a chemical cross-linker mainly in the latter. Poly(acrylic acid) (PAA)-gelatin-GO nanocomposite hydrogels were reported [19], which were synthesized by *in situ* polymerization of acrylic acid monomer in the presence of GO and gelatin. The hydrogels exhibited a 71% increase in tensile strength (150–250 kPa) when containing 90 wt% water, by the addition of 0.3 wt% GO [19]. The same group reported that PAA-gelatin-GO nanocomposite hydrogels with different compositions showed a high compressive strength (7–26 MPa) at a water content of 29–51 wt% [20]. Gelatin methacrylate-GO composite

hydrogels, which exhibited a fracture strength in compression of 91–501 kPa with 94.3–94.5 wt% water, were also reported [21].

Using N,N-methylenebisacrylamide (BIS) as the chemical cross-linker in the presence of GO sheets, tough GO-based polyacrylamide (PAM) composite hydrogels were synthesized by *in situ* polymerization of acrylamide monomers [22]. By incorporating GO sheets, the hydrogels were double cross-linked with the predominant cross-linking contribution from BIS and the additional contribution from multifunctional cross-linking agents of GO sheets, imparting high toughness and a tensile strength of 30 kPa. Actuator materials based on PAM-GO composite hydrogels were prepared by a similar method by others [23]. As the authors suggested that PAM macromolecules grafted onto the GO nanosheets during polymerization, the double cross-linked structure was obtained in the hydrogels which were cross-linked by BIS and GO nanosheets. The good dispersion of the GO nanosheets in the composite hydrogels, resulting from some PAM macromolecules grafted onto the GO nanosheets, endows significant improvement of their mechanical properties, *i.e.*, a 6-fold increase in the compressive strength with 1 wt% GO content in comparison to that of neat PAM hydrogel. These imply double cross-linking polymer hydrogels could be an effective strategy to develop polymer hydrogels with high mechanical properties, like in the case of double cross-linked polymer blend hydrogels [24].

In this work, we developed novel double cross-linked gelatin-GO nanocomposite hydrogels with various weight ratios prepared using cross-linking agents of glutaraldehyde (GTA) and GTA-grafted GO. The nanocomposite hydrogels were characterized with different techniques and discussed with regards to their chemical structures, morphologies, and mechanical properties in detail.

## 2. Experimental section

### 2.1 Materials

Gelatin (type B, BioReagent, bloom strength 225, number average molecular weight: 50,000), graphite powder (size < 20  $\mu\text{m}$ ), potassium permanganate, sodium nitrate, hydrogen peroxide (30%), concentrated sulphuric acid (98%), hydrochloric acid (35%), glutaraldehyde (50%), and glycine ( $1 \text{ mol L}^{-1}$ ) were all obtained from Sigma-Aldrich Corporation.

### 2.2 Preparation of gelatin-GO hydrogels

Graphene oxide was prepared from pristine graphite powder by a modified Hummers' method [25], and purified and freeze-dried [17]. The gelatin-GO nanocomposite hydrogels were synthesized by cross-linking gelatin using GTA in the presence of GO nanosheets. A typical synthesis of the gelatin-GO nanocomposite hydrogel is described as follows. 0.1 mL of aqueous GTA ( $0.056 \text{ g}$ ,  $0.56 \text{ mg mL}^{-1}$ ) solution was mixed with 4.9 mL of aqueous GO ( $0.001 \text{ g}$ ,  $0.2 \text{ mg mL}^{-1}$ ) suspension under vigorous stirring at  $37 \text{ }^\circ\text{C}$  for 1 h.  $0.999 \text{ g}$  gelatin was added into 5 mL distilled water and then heated at  $60 \text{ }^\circ\text{C}$  while stirring for 1 h. It was then added into the water mixture of GTA and GO under stirring for 3 min before it was cast into a cylindrical mould. The mixture was kept at room temperature ( $20 \text{ }^\circ\text{C}$ ) for 24 h to complete the gelation of gelatin through chemical cross-linking. In these hydrogels, GO concentration increased from 0 to  $5 \text{ mg mL}^{-1}$ , while the weight ratio of both gelatin and GO to water was kept constant at 1:10. After gelation, the remaining aldehyde groups from GTA were blocked by immersing the bulk hydrogel into a glycine solution ( $100 \text{ mM}$ ) at  $37 \text{ }^\circ\text{C}$  for 1 h, and following triple wash in distilled water. The hydrogels were named as GH $n$ , in which  $n$  denoted ten times of the concentration ( $\text{mg mL}^{-1}$ ) of GO in the final hydrogel.

### **2.3 Structure characterization**

Gelatin, GO and gelatin-GO hydrogels were analyzed by Fourier transform infrared spectroscopy (FT-IR) (Perkin Elmer Spectrum 100, a resolution of  $4.0\text{ cm}^{-1}$ ). An aqueous GO suspension and the nanocomposite hydrogels were frozen at  $-20\text{ }^{\circ}\text{C}$ , and then dried under vacuum at  $-10\text{ }^{\circ}\text{C}$  for two days by using a FreeZone Triad Freeze Dry System (Labconco Corporation). As a control sample to study the interactions between GO and GTA, the GTA-modified GO was also investigated by FT-IR. This sample was prepared using the same procedure as for nanocomposite hydrogel, namely mixing the same amount of GO suspension and GTA solution at  $37\text{ }^{\circ}\text{C}$  for 1 h, followed by dialysis for 3 days to remove the unreacted GTA and then air-dry at room temperature for 3 days. A neat GO suspension was also air-dried and characterized as a control. Morphologies of the gelatin-GO hydrogels were studied by using scanning electron microscopy (SEM). The lyophilized samples were fractured and then fixed on aluminium stubs. Samples were gold coated by using an Emscope SC500A sputter coater before the morphological images were taken under an FEI Inspect F scanning electron microscope. The average pore sizes were calculated (at least 100 pores) by using ImageJ software.

### **2.4 Compression tests**

Uniaxial compression testing was performed using a mechanical testing system (Model TA500, Lloyd Instruments) equipped with a control and analysis software of NEXYGEN. The hydrogel rods (20 mm high and 10 mm in diameter) were compressed at a speed rate of  $1\text{ mm min}^{-1}$  using a 50 N load cell. Measurements were performed on 5 replicate samples in each group.

## 2.5 Rheological measurements

The rheological properties were measured by using a MCR 301 rheometer (Anton Paar). The shear moduli were recorded against angular frequency with a fixed strain of 0.1% (within the linear viscoelastic region) at room temperature. Parallel-plate (diameter 25 mm) geometry was used and the gap distance was fixed (2.0 mm) between the parallel plates.

## 2.6 Swelling tests

Hydrogel discs ( $10 \times 10 \times 2 \text{ mm}^3$ ) were air-dried for one week at room temperature and then submerged in distilled water at room temperature ( $23 \pm 1 \text{ }^\circ\text{C}$ ) for swelling test. The samples were weighed after a week when the weights became constant. Three replicate samples were used for the measurements. The swelling ratio (SR) of the hydrogel was calculated using equation 1:

$$SR = \frac{W_s - W_d}{W_d} \quad (1)$$

in which  $W_s$  and  $W_d$  denote the weights of the swollen and dried hydrogel, respectively.

## 3. Results and discussion

GO nanosheets used to synthesize the nanocomposite hydrogels have been characterized by atomic force microscopy (AFM) and laser sizing in our previous works [17]. The thickness of single-layer GO nanosheets was determined to be 1.0 nm and the majority of GO nanosheets ranged in size from 2.2 to 20  $\mu\text{m}$  with a mean of 5.5  $\mu\text{m}$  [17]. When a GO aqueous suspension was utilized for the preparation of GO reinforced hydrogels, the functional groups on the GO nanosheets provided sites for physical and chemical interactions with the polymer matrix [26,27].

As described before [28], the spectrum of GO (curve a in Fig. 1(A)) shows the existence of different oxygen-containing functional groups: carbonyl groups ( $\text{C}=\text{O}$ ,  $1729 \text{ cm}^{-1}$ ), alkoxy groups ( $\text{C}-\text{O}$ ,  $1044 \text{ cm}^{-1}$ ) and epoxy groups ( $\text{C}-\text{O}-\text{C}$ ,  $1222 \text{ cm}^{-1}$ ). O-H stretching bond and

C=C vibrations are also observed at 3200-3400  $\text{cm}^{-1}$  and 1616  $\text{cm}^{-1}$ , respectively. Gelatin is characterized for comparison, and its main characteristic groups are identified in curve h. The absorption bands at 1633, 1522, 1230 and 3285  $\text{cm}^{-1}$  are assigned to the amide I vibration (C=O), amide II bending vibration (N-H), amide III and N-H stretching, respectively [29]. GH0 has a similar profile to gelatin powder. After incorporation of GO into the gelatin, the C=O peak in GO at 1729  $\text{cm}^{-1}$  disappears in the gelatin-GO nanocomposite (curve b-g), which is ascribed to the association between carboxyl groups on GO nanosheets and amino functional groups in gelatin to form ammonium carboxylate complex [30]. The features of the amide I vibration and amide II bending vibration from gelatin dominate in the studied nanocomposites (curves b-g), overshadowing the feature of C=C vibrations from GO.

To investigate the formation mechanism of the hydrogels further, the FT-IR spectrum of the mixture of GO and GTA, prior to mixing with gelatin solution to form a hydrogel, was also studied. Fig. 1(B) shows the spectra comparison of GO and GTA modified GO. The occurrence of a new shoulder at 2792-2840  $\text{cm}^{-1}$ , which corresponds to the C-H stretch mode of GTA, initially indicates the presence of GTA on GO sheets. The peaks of C-O and C-O-C show some shifts from 1046 and 1214 to 1056  $\text{cm}^{-1}$  and 1224  $\text{cm}^{-1}$  respectively, as well as significant increases of their intensities, suggesting the formation of hemiacetal structure by reacting the hydroxyl groups of GO sheets with aldehyde groups of GTA [31]. The C=O peak at 1720  $\text{cm}^{-1}$  shifts to 1704  $\text{cm}^{-1}$  and its intensity increases, which is ascribed to the residual unreacted aldehyde groups of GTA as its one end may still remain free while the other end reacts with GO. These findings are in line with those reported in the literature [31], confirming the reaction between the hydroxyl groups of GO and the aldehyde groups of GTA and their covalent bonding. The proposed chemical reaction is illustrated in Scheme 1. The remaining aldehyde groups on the GTA modified GO act as multiple cross-linker points for further reaction with gelatin chains during hydrogel gelation. It is known that the aldehyde

groups of GTA react with amino groups in gelatin to yield Schiff bases [32] and cross-link gelatin molecular chains to create a network. Additional cross-linking was also reported through the reaction between aldehyde groups of GTA and hydroxyl groups of gelatin [32]. Thus, the gelatin-GO nanocomposite hydrogels are formed through double cross-linking by GTA molecules and GTA modified multifunctional GO sheets, and possibly also with additional physical interactions, including electrostatic interaction and hydrogen bonding, between the carboxyl, epoxy and unreacted hydroxyl groups on GO nanosheets and amino groups in gelatin molecules. The mechanism of the formation of double cross-linked structure in the gelatin-GO nanocomposite hydrogel is proposed in Scheme 2.

The interior morphologies of the double cross-linked gelatin-GO nanocomposite hydrogels were investigated by SEM. The neat gelatin hydrogel cross-linked by GTA, GH0, displayed a porous structure with a pore size of  $1.67 \pm 0.38 \mu\text{m}$  (Fig. 2(A)). After incorporation of GO, the gelatin-GO hydrogel is double cross-linked by both GTA and GTA-grafted GO and becomes stiffer, which suppresses the growth of ice crystals during the freezing step. This resulted in a smaller pore size for gelatin-GO hydrogel GH1 ( $0.74 \pm 0.29 \mu\text{m}$ ) with a narrow pore size distribution (Fig. 2(B)), suggesting good distribution of GO sheets within the hydrogel at the low concentration. With increasing GO, the pores become uneven and shallower (Fig. 2C-F). A wider distribution of pore sizes suggests GO is not well distributed in localized areas of the hydrogel network. GH5, GH10, GH30 and GH50 have bigger average pore sizes of  $0.89 \pm 0.35 \mu\text{m}$ ,  $1.21 \pm 0.42 \mu\text{m}$ ,  $1.38 \pm 0.66 \mu\text{m}$  and  $1.27 \pm 0.44 \mu\text{m}$ , respectively.

Mechanical properties of the double cross-linked gelatin-GO hydrogels were evaluated by uniaxial compression. The compressive strength of the hydrogel increases upon the increase of the GO concentration (Fig. 3(A)). The compressive strength of 566 kPa for GH50 with the highest GO concentration shows a 288% increase compared to 146 kPa for the neat gelatin

hydrogel (Table 1). These values are comparable to those values (91–501 kPa) of gelatin methacrylate-GO composite hydrogels [21]. The compressive modulus of the gelatin-GO nanocomposite hydrogel increases in general upon the incorporation of GO into the hydrogel. It records the maximum modulus of 62 kPa for GH30 which almost triples the value (21 kPa) of the neat gelatin hydrogel (Table 1). These significant improvements in the mechanical properties of the gelatin hydrogel are attributed to the double cross-linked network structure in the nanocomposite hydrogels in which GO sheets, grafted with GTA, act as multifunctional cross-linkers, and also to the reinforcement effect of GO as an effective nanofiller, with a high fracture strength, Young's modulus over 208 GPa [33], a high aspect ratio and a large surface area. Furthermore, carboxyl, epoxy and unreacted hydroxyl groups on the GO nanosheets are well associated with the polar gelatin by electrostatic interaction and hydrogen bonding [17,34], also providing effective load transfer between gelatin matrix and GO nanosheets in addition to the covalent bonds. The compressive fracture energies (the areas under the compressive stress-strain curves) of the nanocomposite hydrogels are also calculated and shown in Table 1, increasing from 20.8 kJ m<sup>-3</sup> for GH0 to 76.3 kJ m<sup>-3</sup> for GH50. The high flexibility and mobility of GO nanosheets can help effectively dissipate energy that is applied to the hydrogel, and therefore has a prominent effect on the hydrogel toughness [35,36].

The compressive tangent moduli of the hydrogels significantly varied upon the change of strain magnitude, indicating nonlinear and viscoelastic material behavior (Fig. 3(B)). The tangent moduli of all gelatin-GO hydrogels are higher than those of the neat gelatin hydrogel at strain magnitudes greater than 10%. The tangent modulus of GH30 is higher than that of GH50 at strain magnitudes greater than 10%, in line with their compressive moduli. This may be due to the poorer dispersion of GO sheets in GH50. The content of GO sheets has two opposing effects on modulus: on one side, a higher GO content increases the modulus of the

hydrogel; but on the other side, it causes poorer dispersion which leads to aggregation of some GO sheets and so overall reduces the cross-linking density and the modulus. In contrast, the compressive strains at break of gelatin-GO hydrogels are all similar except for GH5. Overall, the compressive strength, stiffness and toughness of the gelatin hydrogel are improved by the presence of GO, which plays a critical role in enhancing their mechanical properties.

Rheological measurements (Fig. 4) reveal viscoelastic characteristics of the hydrogels. Their storage moduli ( $G'$ ) are always greater than their counterpart loss moduli ( $G''$ ), indicating elastic behavior is dominant in these hydrogels [37]. In Fig. 4(A),  $G'$  is about one to two magnitude orders higher than its corresponding  $G''$  (Fig. 4(B)). So, the values of the damping factor,  $\tan \delta$  ( $\tan \delta = G''/G'$ ), are much lower than 1, suggesting the formation of highly elastic hydrogels (Fig. 4(C)) [38]. The storage modulus of the neat gelatin hydrogel (GH0) is 10.4 kPa (at 10 rad s<sup>-1</sup>). With the incorporation of GO into the gelatin hydrogels, their storage modulus increases. A 12% increase has been observed in the hydrogel GH1 (11.6 kPa), compared to that of GH0. The storage modulus of GH10 (20.1 kPa) increases more significantly, showing 93% increase in contrast to GH0. The storage modulus reaches the highest value of 27.0 kPa (at 10 rad s<sup>-1</sup>) for GH30 which shows a 160% increase, though it is lower than that of GH50 below the crossover point at 2 rad s<sup>-1</sup>. A further increase in the concentration of GO leads to a decline in the storage modulus to 23.6 kPa (at 10 rad s<sup>-1</sup>) for GH50, indicating the structure weakening, which may be owing to the aggregation of GO and a lower cross-linking density as previously discussed.

The cross-linking density ( $N$ ) of the hydrogels, an important parameter to characterize the structure-property relationship of hydrogels, was investigated. It is useful for the design of the new hydrogels and manipulation of their properties.  $N$  is defined as the number of active network chains per volume of the hydrogel. A cross-linked hydrogel can be considered as a

Gaussian network and  $N$  is related to the static shear modulus ( $G$ ) [39]. The correlation between them was described by the rubber elasticity theory, as shown in equation 2 [39],

$$G = NkT = \frac{cRT}{\overline{M}_c} \left(1 - \frac{2\overline{M}_c}{\overline{M}}\right) \quad (2)$$

in which  $k$  is Boltzmann constant,  $T$  is absolute temperature (298 K),  $R$  is the gas constant,  $c$  is the concentration of the polymer (gelatin),  $\overline{M}_c$  is the average molecular weight of polymer chain segments between the cross-linking sites, and  $\overline{M}$  is the molecular weight of the polymer. In the literature, an empirical correlation [40] between dynamic Young's modulus and static Young's modulus and a correlation [41] between shear modulus and Young's modulus were reported. As a result, the static shear modulus was related to dynamic shear modulus in equation 3 [17,18],

$$G = 0.629G' - \frac{1.586}{2(1+\nu)} \quad (3)$$

where  $\nu$  is Poisson's ratio, which is determined as 0.5 [42]. By substituting the experimental data of  $G'$  in equations 2 and 3, the parameters are calculated and illustrated in Table 2.

The cross-linking density,  $N$ , of the hydrogel increases with the increase in the GO concentration, from  $15.9 \times 10^{23} \text{ m}^{-3}$  for GH0 up to  $41.3 \times 10^{23} \text{ m}^{-3}$  for GH30 before dropping to  $36.1 \times 10^{23} \text{ m}^{-3}$  for GH50. The hydrogel with a higher modulus possesses a higher cross-linking density, which is consistent with the literature [17,43]. Considering the same amount of chemical cross-linker (GTA) was used in the synthesis of hydrogels, it is GO that induces the higher cross-linking density; it acts as both a multifunctional cross-linker, when grafted with multiple GTA, and a reinforcing nanofiller. Like the case with compressive or storage modulus, the decrease of  $N$  for GH50, which has the highest GO content, can be explained by less effective cross-links between GO nanosheets and gelatin molecules due to increased aggregation of GO sheets. The values of  $\overline{M}_c$  obtained vary in reverse to the cross-linking

density, decreasing from 15,057 to 9,210 g mol<sup>-1</sup> for GH0 and GH30 respectively before increasing to 10,006 g mol<sup>-1</sup> for GH50.

To better understand the influence of GO on the cross-linking of the hydrogels, the swelling property of the lyophilized gelatin-GO nanocomposite hydrogels with different amounts of GO was measured, and the results are shown in Fig. 5. The swelling reached equilibrium in distilled water after a week. All the hydrogels basically maintained their original shape, and no migration of GO nanosheets from the hydrogel into water was observed during the swelling process. With the increase of the amount of GO, the swelling ratio of gelatin-GO nanocomposite generally decreases. The equilibrium swelling ratio decreases from 8.3 g g<sup>-1</sup> for GH0 to 7.4 g g<sup>-1</sup> for GH50. This confirms a higher cross-linking degree in the nanocomposite hydrogel. More specifically, GO sheets, grafted with multiple GTA, can function as multifunctional cross-linking agents to form multiple junctions in the network and inhibit their swelling, resulting in the decrease in swelling capacity. Similar phenomena have been reported for different nanofiller-enhanced hydrogels in the literature [44,45]. However, the swelling ratio (7.4 g g<sup>-1</sup>) of GH50 is higher than that (7.0 g g<sup>-1</sup>) of GH30 presumably due to increased aggregation of GO sheets. It is well known that there is a strong correlation between the swelling capacity and the effective cross-link density of the hydrogels. Thus, the effective cross-linking density of GH50 is lower than that of GH30. The results are in line with the corresponding cross-linking densities derived from mechanical properties and presented in the Table 2.

These gelatin-GO nanocomposite hydrogels may be fabricated into different shapes or forms for future applications. For example, they could be cast onto moulds with different shapes and dimensions to form complex 3D objects, and fabricated into fibres and nonwoven fibrous constructs using gyratory methods [46,47].

## **4. Conclusions**

Double cross-linked gelatin-GO nanocomposite hydrogels have been successfully synthesized by using both GTA and GTA modified GO sheets as cross-linking agents. The hydrogels with varying amount of GO display the improved mechanical strength, stiffness and toughness, which is ascribed to the double cross-linked network structure and also the contribution of GO sheets as multifunctional cross-linkers and effective reinforcing nanofillers. At a fixed GTA concentration, the compressive strength of the hydrogel increases with increasing GO content. GH50, containing 5 mg mL<sup>-1</sup> GO, shows the highest compressive strength of 566 kPa at a strain of 70%, exhibiting a 288% increase compared to the neat gelatin hydrogel. However, the highest elastic modulus of 62 kPa is observed for GH30 with 3 mg mL<sup>-1</sup> GO, which has a compressive strength of 509 kPa at a strain of 65.9%. The elastic modulus value of GH30 doubles that of the neat gelatin hydrogel. The shear storage modulus of the hydrogel generally increases with the increase in GO content, apart from the highest GO content. The highest value of shear storage modulus is 27.0 kPa for GH30, showing a 160% increase to 10.4 kPa for GH0. The swelling capacity of gelatin-GO hydrogel decreases with the increase in the cross-link degree and mechanical properties of the hydrogel. The novel nanocomposite hydrogels could have the potential to be used in biomedical engineering.

## **Acknowledgements**

The authors thank the British Council and the Department of Business, Innovation and Skills for a Global Innovation Initiative grant (GII207).

## **References**

- [1] N. Annabi, J.W. Nichol, X. Zhong, C. Ji, S. Koshy, A. Khademhosseini, F. Deghani, Controlling the porosity and microarchitecture of hydrogels for tissue engineering, *Tissue Eng. Part B* 16 (2010) 371-383.
- [2] K. Madhumathi, K.T. Shalumon, V.V.D. Rani, H. Tamura, T. Furuike, N. Selvamurugan, S.V. Nair, R. Jayakumar, Wet chemical synthesis of chitosan hydrogel-hydroxyapatite composite membranes for tissue engineering applications, *Int. J. Biol. Macromolec.* 45 (2009) 12-15.
- [3] H. Li, L. Zhao, X.D. Chen, R. Mercadé-Prieto, Swelling of whey and egg white protein hydrogels with stranded and particulate microstructures, *Int. J. Biol. Macromolec.* 83 (2016) 152-159.
- [4] D. Liu, M. Nikoo, G. Boran, P. Zhou, J.M. Regenstein, Collagen and gelatin, *Annu. Rev. Food Sci. Technol.* 6 (2015) 527-557.
- [5] S. Young, M. Wong, Y. Tabata, A.G. Mikos, Gelatin as a delivery vehicle for the controlled release of bioactive molecules, *J. Controlled Release* 109 (2005) 256-274.
- [6] N.C. Hunt, L.M. Grover, Cell encapsulation using biopolymer gels for regenerative medicine, *Biotechnol. Lett.* 32 (2010) 733-742.
- [7] D. Hellio, M. Djabourov, Physically and chemically crosslinked gelatin gels, *Macromol. Symp.* 241 (2006) 23-27.
- [8] J.E. Eldridge, J.D. Ferry, Studies of the cross-linking process in gelatin gels. III. Dependence of melting point on concentration and molecular weight, *J. Phys. Chem.* 58 (1954) 992-995.
- [9] C. Wu, C.-Y. Yan, Studies of the swelling and drying kinetics of thin gelatin gel films by in situ interferometry, *Macromolecules* 27 (1994) 4516-4520.
- [10] S. Naficy, H.R. Brown, J.M. Razal, G.M. Spinks, P.G. Whitten, Progress toward robust polymer hydrogels, *Aust. J. Chem.* 64 (2011) 1007-1025.
- [11] A.M. Costa, J.F. Mano, Extremely strong and tough hydrogels as prospective candidates for tissue repair—A review, *Eur. Polym. J.* 72 (2015) 344-364.
- [12] H. Kim, A.A. Abdala, C.W. Macosko, Graphene/polymer nanocomposites, *Macromolecules* 43 (2010) 6515-6530.

- [13] Y. Zhu, S. Murali, W. Cai, X. Li, J.W. Suk, J.R. Potts, R.S. Ruoff, Graphene and graphene oxide: Synthesis, properties, and applications, *Adv. Mater.* 22 (2010) 3906-3924.
- [14] A. Amir, S. Mahalingam, X. Wu, H. Porwal, P. Colombo, M.J. Reece, M. Edirisinghe, Graphene nanoplatelets loaded polyurethane and phenolic resin fibres by combination of pressure and gyration, *Compos. Sci. Technol.* 129 (2016) 173-182.
- [15] X. Ma, Y. Li, W. Wang, Q. Ji, Y. Xia, Temperature-sensitive poly(*n*-isopropylacrylamide)/graphene oxide nanocomposite hydrogels by in situ polymerization with improved swelling capability and mechanical behavior, *Eur. Polym. J.* 49 (2013) 389-396.
- [16] C. Wan, M. Frydrych, B. Chen, Strong and bioactive gelatin-graphene oxide nanocomposites, *Soft Matter* 7 (2011) 6159-6166.
- [17] Y. Piao, B. Chen, Self-assembled graphene oxide-gelatin nanocomposite hydrogels: Characterization, formation mechanisms, and pH-sensitive drug release behavior, *J. Polym. Sci. Part B: Polym. Phys.* 53 (2015) 356-367.
- [18] Y. Piao, B. Chen, One-pot synthesis and characterization of reduced graphene oxide-gelatin nanocomposite hydrogels, *RSC Adv.* 6 (2016) 6171-6181.
- [19] S. Faghihi, A. Karimi, M. Jamadi, R. Imani, R. Salarian, Graphene oxide/poly(acrylic acid)/gelatin nanocomposite hydrogel: Experimental and numerical validation of hyperelastic model, *Mater. Sci. Eng., C* 38 (2014) 299-305.
- [20] S. Faghihi, M. Gheysour, A. Karimi, R. Salarian, Fabrication and mechanical characterization of graphene oxide-reinforced poly(acrylic acid)/gelatin composite hydrogels, *J. Appl. Phys.* 115 (2014) 083513(1-6).
- [21] S.R. Shin, B. Aghaei-Ghareh-Bolagh, T.T. Dang, S.N. Topkaya, X. Gao, S.Y. Yang, S.M. Jung, J.H. Oh, M.R. Dokmeci, X.S. Tang, Cell-laden microengineered and mechanically tunable hybrid hydrogels of gelatin and graphene oxide, *Adv. Mater.* 25 (2013) 6385-6391.
- [22] J. Shen, B. Yan, T. Li, Y. Long, N. Li, M. Ye, Study on graphene-oxide-based polyacrylamide composite hydrogels, *Composites Part A* 43 (2012) 1476-1481.

- [23] N. Zhang, R. Li, L. Zhang, H. Chen, W. Wang, Y. Liu, T. Wu, X. Wang, W. Wang, Y. Li, Y. Zhao, J. Gao, Actuator materials based on graphene oxide/polyacrylamide composite hydrogels prepared by in situ polymerization, *Soft Matter* 7 (2011) 7231-7239.
- [24] J.P. Gong, Why are double network hydrogels so tough? *Soft Matter* 6 (2010) 2583-2590.
- [25] D.C. Marcano, D.V. Kosynkin, J.M. Berlin, A. Sinitskii, Z.Z. Sun, A. Slesarev, L.B. Alemany, W. Lu, J.M. Tour, Improved synthesis of graphene oxide, *ACS Nano* 4 (2010) 4806-4814.
- [26] Z. Zhao, X. Wang, J. Qiu, J. Lin, D. Xu, C.A. Zhang, M. Lv, X. Yang, Three-dimensional graphene-based hydrogel/aerogel materials, *Rev. Adv. Mater. Sci.* 36 (2014) 137-151.
- [27] S.H. Ku, M. Lee, C.B. Park, Carbon-based nanomaterials for tissue engineering, *Adv. Healthcare Mater.* 2 (2013) 244-260.
- [28] Y.-P. Zhang, J.-J. Xu, Z.-H. Sun, C.-Z. Li, C.-X. Pan, Preparation of graphene and TiO<sub>2</sub> layer by layer composite with highly photocatalytic efficiency, *Prog. Nat. Sci.* 21 (2011) 467-471.
- [29] S. Kim, M.E. Nimni, Z. Yang, B. Han, Chitosan/gelatin-based films crosslinked by proanthocyanidin, *J. Biomed. Mater. Res. Part B* 75 (2005) 442-450.
- [30] S. Park, D.A. Dikin, S.T. Nguyen, R.S. Ruoff, Graphene oxide sheets chemically cross-linked by polyallylamine, *J. Phys. Chem. C* 113 (2009) 15801-15804.
- [31] N. Hu, L. Meng, R. Gao, Y. Wang, J. Chai, Z. Yang, E.S.-W. Kong, Y. Zhang, A facile route for the large scale fabrication of graphene oxide papers and their mechanical enhancement by cross-linking with glutaraldehyde, *Nano-micro Lett.* 3 (2011) 215-222.
- [32] S. Farris, J. Song, Q. Huang, Alternative reaction mechanism for the cross-linking of gelatin with glutaraldehyde, *J. Agric. Food Chem.* 58 (2009) 998-1003.
- [33] J.W. Suk, R.D. Piner, J. An, R.S. Ruoff, Mechanical properties of monolayer graphene oxide, *ACS Nano* 4 (2010) 6557.
- [34] A.B. Bourlinos, D. Gournis, D. Petridis, T. Szabó, A. Szeri, I. Dékány, Graphite oxide: Chemical reduction to graphite and surface modification with primary aliphatic amines and amino acids, *Langmuir* 19 (2003) 6050-6055.

- [35] C. Cha, S.R. Shin, X. Gao, N. Annabi, M.R. Dokmeci, X.S. Tang, A. Khademhosseini, Controlling mechanical properties of cell-laden hydrogels by covalent incorporation of graphene oxide, *Small* 10 (2014) 514-523.
- [36] B. Chen, J.R. Evans, Impact strength of polymer-clay nanocomposites, *Soft Matter* 5 (2009) 3572-3584.
- [37] Y.X. Xu, Q.O. Wu, Y.Q. Sun, H. Bai, G.Q. Shi, Three-dimensional self-assembly of graphene oxide and DNA into multifunctional hydrogels, *ACS Nano* 4 (2010) 7358-7362.
- [38] K. Juby, C. Dwivedi, M. Kumar, S. Kota, H. Misra, P. Bajaj, Silver nanoparticle-loaded PVA/gum acacia hydrogel: Synthesis, characterization and antibacterial study, *Carbohydr. Polym.* 89 (2012) 906-913.
- [39] L.R.G. Treloar, *The physics of rubber elasticity*, Oxford University Press, USA, 1975, pp. 1-2, 160-170.
- [40] J. Sabbagh, J. Vreven, G. Leloup, Dynamic and static moduli of elasticity of resin-based materials, *Dent. Mater.* 18 (2002) 64-71.
- [41] T.K.L. Meyvis, B.G. Stubbe, M.J. Van Steenberghe, W.E. Hennink, S.C. De Smedt, J. Demeester, A comparison between the use of dynamic mechanical analysis and oscillatory shear rheometry for the characterisation of hydrogels, *Int. J. Pharm.* 244 (2002) 163-168.
- [42] C. Macosko, *Rheology: Principles, measurements, and applications*, VCH, New York, 1994, pp. 37-45.
- [43] J. Yang, C.-R. Han, J.-F. Duan, M.-G. Ma, X.-M. Zhang, F. Xu, R.-C. Sun, X.-M. Xie, Studies on the properties and formation mechanism of flexible nanocomposite hydrogels from cellulose nanocrystals and poly(acrylic acid), *J. Mater. Chem.* 22 (2012) 22467-22480.
- [44] W.-C. Lin, W. Fan, A. Marcellan, D. Hourdet, C. Creton, Large strain and fracture properties of poly(dimethylacrylamide)/silica hybrid hydrogels, *Macromolecules* 43 (2010) 2554-2563.
- [45] S. Das, F. Irin, L. Ma, S.K. Bhattacharia, R.C. Hedden, M.J. Green, Rheology and morphology of pristine graphene/polyacrylamide gels, *ACS Appl. Mater. Interfaces* 5 (2013) 8633-8640.
- [46] S. Mahalingam, M. Edirisinghe, Forming of polymer fibres by a pressurised gyration process, *Macromol. Rapid Commun.* 34 (2013) 1134-1139.

- [47] Z. Xu, S. Mahalingam, P. Basnett, B. Raimi-Abraham, I. Roy, D. Craig, M. Edirisinghe, Making nonwoven fibrous poly( $\epsilon$ -caprolactone) constructs for antimicrobial and tissue engineering applications by pressurized melt gyration, *Macromol. Mater. Eng.* 301 (2016) 922-934.

**Table 1**

Compressive properties of the double cross-linked gelatin-GO nanocomposite hydrogels.

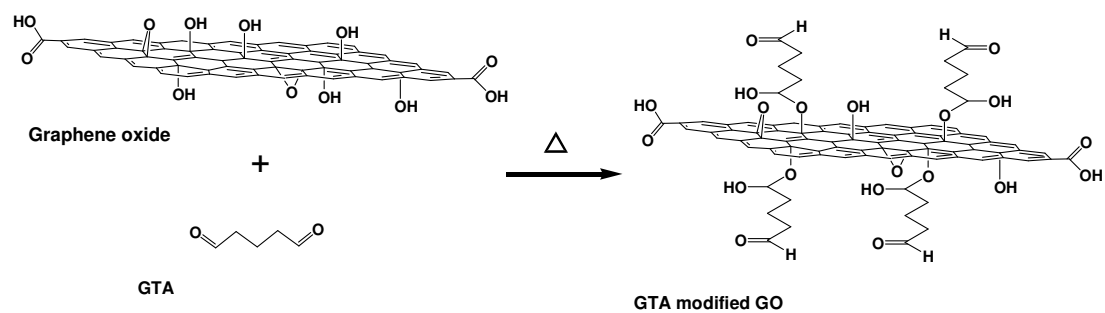
Sample	Compressive strength (kPa)	Young's modulus (kPa)	Fracture strain (%)	Fracture energy (kJ m <sup>-3</sup> )
GH0	146 ± 11	21 ± 10	67.9 ± 4.4	20.8 ± 14.9
GH1	286 ± 25	31 ± 12	67.5 ± 11.4	37.3 ± 4.4
GH5	253 ± 55	31 ± 14	77.0 ± 4.4	40.9 ± 6.0
GH10	377 ± 68	42 ± 9	70.2 ± 2.4	49.7 ± 6.7
GH30	509 ± 118	62 ± 18	65.9 ± 5.0	74.2 ± 20.7
GH50	566 ± 56	58 ± 11	70.0 ± 2.5	76.3 ± 4.7

**Table 2**

$N$  and  $\overline{M}_c$  in the double cross-linked gelatin-GO nanocomposite hydrogels with different compositions.

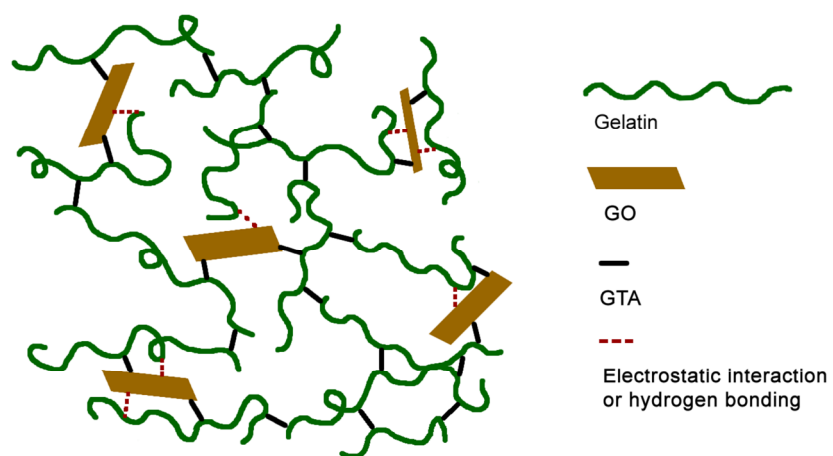
Sample	Gelatin (wt.%)	GO (mg mL <sup>-1</sup> )	GTA (g)	$G'$ (kPa)	$N$ ( $\times 10^{23}$ m <sup>-3</sup> )	$\overline{M}_c$ (g mol <sup>-1</sup> )
GH0	10	0	0.056	10.4	15.9	15057
GH1	10	0.1	0.056	11.6	17.7	14396
GH5	10	0.5	0.056	10.8	16.5	14830
GH10	10	1	0.056	20.1	30.7	10983
GH30	10	3	0.056	27.0	41.3	9210
GH50	10	5	0.056	23.6	36.1	10006

## Scheme 1



**Scheme 1.** The proposed chemical reaction between GO and GTA.

## Scheme 2



**Scheme 2.** The proposed schematic structure of double cross-linked gelatin-GO nanocomposite hydrogels. Here, double cross-linkers refer to GTA and GTA-modified GO. As the physical interactions are weaker than the two chemical cross-links, they are not considered in the term of double cross-links.

## Figure captions

**Fig. 1.** (A) FT-IR spectra of the lyophilized (a) GO, (b) GH0, (c) GH1, (d) GH5, (e) GH10, (f) GH30, (g) GH50, and (h) neat gelatin; (B) FT-IR spectra comparison of (a) GO and (b) GTA surface-modified GO.

**Fig. 2.** SEM images of lyophilized gelatin-GO nanocomposite hydrogels: (a) GH0, (b) GH1, (c) GH5, (d) GH10, (e) GH30 and (f) GH50.

**Fig. 3.** (A) Compressive stress-strain curves and (B) compressive tangent modulus versus compressive strain of hydrogels: GH0, GH1, GH5, GH10, GH30 and GH50.

**Fig. 4.** (A)  $G'$  (solid), (B)  $G''$  (hollow) and (C) damping factor  $\tan \delta$  of hydrogels: GH0, GH1, GH5, GH10, GH30 and GH50.

**Fig. 5.** Equilibrium swelling of the double cross-linked gelatin-GO nanocomposite hydrogels with various GO contents: GH0, GH1, GH5, GH10, GH30 and GH50.

**Scheme 1.** The proposed chemical reaction between GO and GTA.

**Scheme 2.** The proposed schematic structure of double cross-linked gelatin-GO nanocomposite hydrogels. Here, double cross-linkers refer to GTA and GTA-modified GO. As the physical interactions are weaker than the two chemical cross-links, they are not considered in the term of double cross-links.

Fig. 1

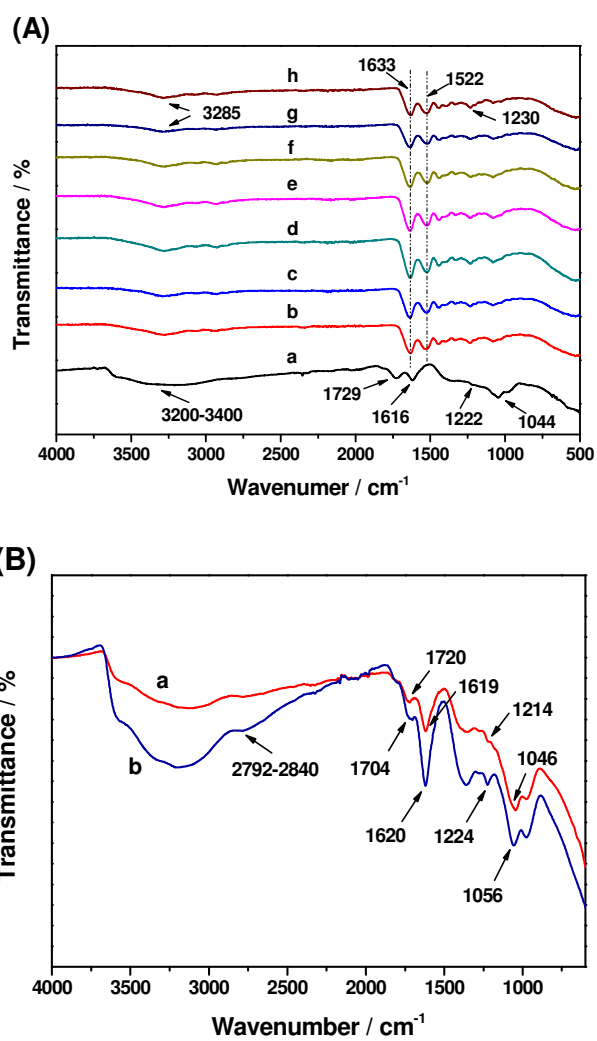


**Fig. 2**

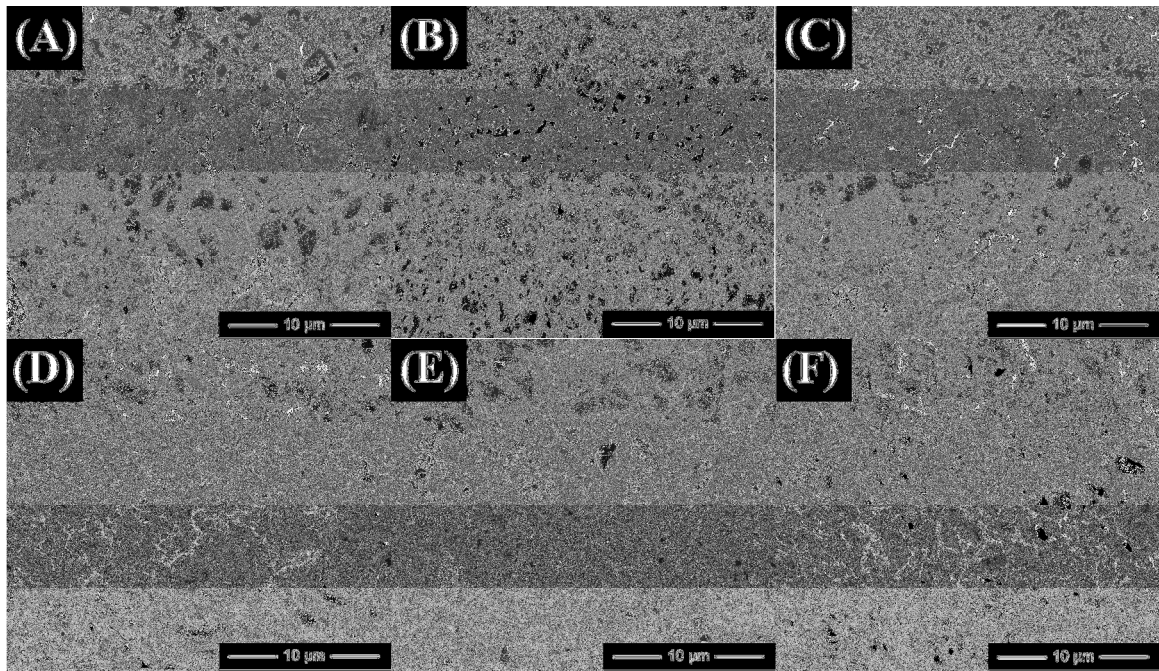


Fig. 3

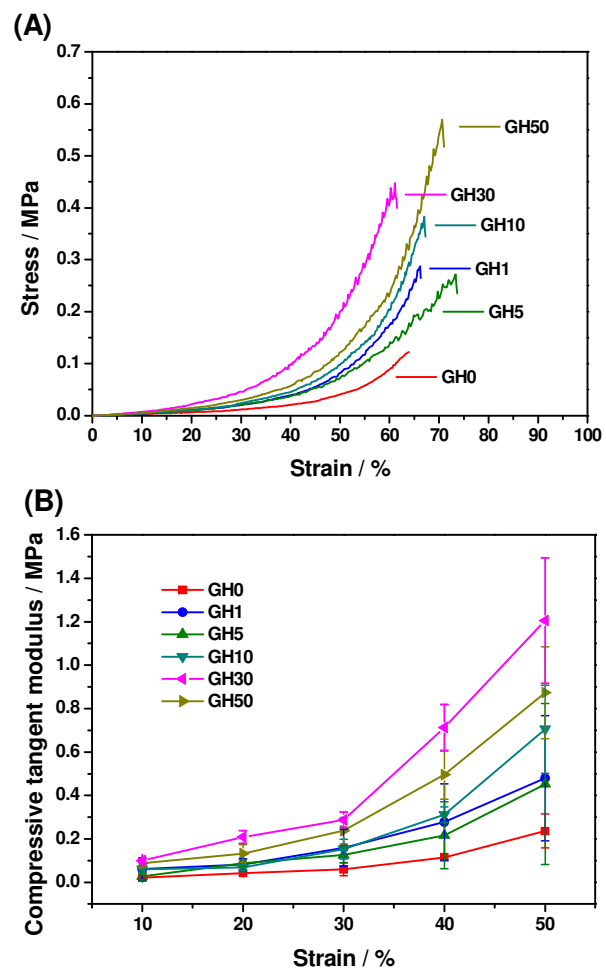
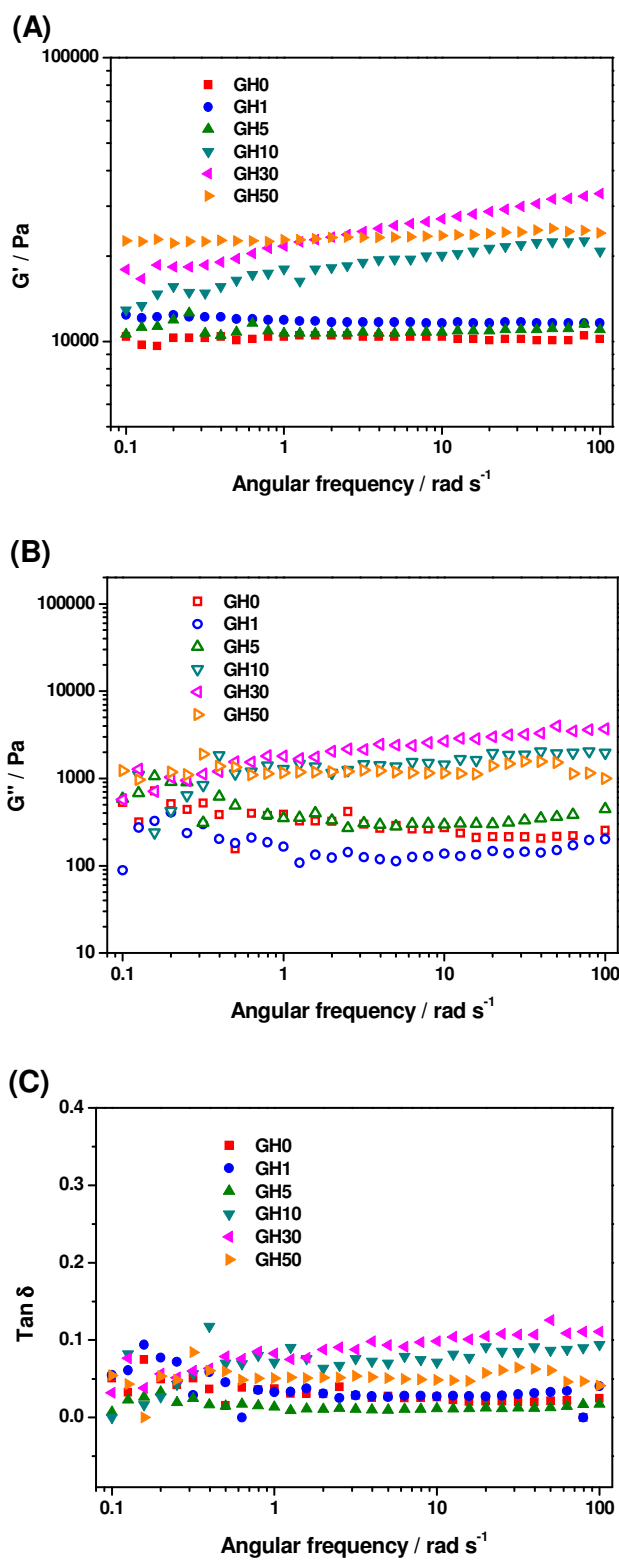


Fig. 4



**Fig. 5**

